

# Fluctuations in ion channel gating currents

## Analysis of nonstationary shot noise

S. C. Crouzy and F. J. Sigworth

Department of Cellular and Molecular Physiology, Yale University School of Medicine, New Haven, Connecticut 06510 USA

**ABSTRACT** Conti and Stühmer (1989, *Eur. Biophys. J.* 17:53–59) have measured the nonstationary shot noise in the gating current of a population of sodium channels. Here we present expressions for the autocovariance and variance of such noise from general Markov models of channel kinetics, based on the theoretical work of E. Frehland. We compare the predictions of the independent, two-state gating model used by Conti and Stühmer with a six-state model of sodium channel activation based on the work of Armstrong and Gilly (1979, *J. Gen. Physiol.* 74:691–711). We find that Conti and Stühmer's experiment would not be able to distinguish between these schemes. We describe experimental conditions under which better model discrimination would be possible.

### INTRODUCTION

Voltage-sensitive gating in an ion channel appears to occur as transitions among discrete conformational states of the channel. The gating current, which reflects the movement of charged structures during these transitions, is therefore expected to consist of discrete, sudden charge movements. If it were possible to measure these individual impulses of current, one would obtain direct information about the individual kinetic steps and the intramembranous charge displacements that accompany them (Fig. 1). The individual charge movements in a single channel are not presently observable because they are expected to be at most a few elementary charges in magnitude. In an experimental *tour de force* Conti and Stühmer (1989) have however recorded fluctuations in the gating current from thousands of channels in a membrane patch from a *Xenopus* oocyte injected with cRNA for the Rat Brain II sodium channel clone. The fluctuations are of the expected magnitude for "shot noise" arising from discrete charge movements, and in fact give an estimate of the magnitude of the charge movement in individual conformational steps leading to channel opening.

Conti and Stühmer interpreted their data in terms of a theory for the variance from a two-state model of the charge movement process; in their analysis the effect of filtering on the variance was incorporated as an approximation. In this paper we extend their theory to discrete kinetic schemes of arbitrary complexity, and present the exact solution and approximations for the effects of filtering. We compare the predictions of the two-state model with a representative alternative theory, the six-state model of the activation process in squid sodium channels of Armstrong and Gilly (1979).

### THEORY

Frehland (1978, 1982) has presented a theory for stationary fluctuations in discrete charge-transport systems, which has been applied in studies of transport noise in open channels (e.g., Heinemann and Sigworth, 1990). Since gating currents are displacement currents that flow transiently after a change in membrane potential, a

theory for nonstationary fluctuations is required. The extension of the theory to the nonstationary case is straightforward: Frehland (1982) presented the expression for the autocovariance (our Eq. 10) without further discussion, noting however that "... presently it is doubtful if a sensible experimental analysis can be performed." In view of the theory's clear applicability to the study of channel gating currents, we summarize its derivation here. We change the notation however to conform to the standard "Q-matrix" description of channel gating (Colquhoun and Hawkes, 1977).

Let  $I(t)$  be the random, time-dependent gating current from one channel, and represent its expectation value (averaged over an ensemble of trials) as

$$\mu(t) = \langle I(t) \rangle.$$

Also, from an ensemble of trials one can compute the nonstationary autocovariance function

$$C(t_1, t_2) = \langle [I(t_1) - \mu(t_1)][I(t_2) - \mu(t_2)] \rangle, \quad (1)$$

which relates fluctuations in the gating current, about the mean, at one time  $t_1$  with those at another time  $t_2$ . It is also possible to write the autocovariance in the form

$$C(t_1, t_2) = \langle I(t_1)I(t_2) \rangle - \mu(t_1)\mu(t_2). \quad (2)$$

The variance  $\sigma^2$  of the fluctuations, which is also time dependent, is obtained from the covariance as

$$\sigma^2(t) = C(t, t).$$

### Gating current

Let us now consider a kinetic scheme representing the  $n$  states of a single channel. Using the notation of Colquhoun and Hawkes (1977), we let  $q_{ij}$  be the transition rate from state  $i$  to state  $j$ . The time evolution of the probabilities  $p_j$  is then obtained as the solution of the equation

$$\frac{d\mathbf{p}(t)}{dt} = \mathbf{p}(t)\mathbf{Q}, \quad (3)$$

where  $\mathbf{p}$  is the row vector of probabilities and  $\mathbf{Q}$  is the matrix of transition rates, with the diagonal elements chosen to make each row sum to zero.

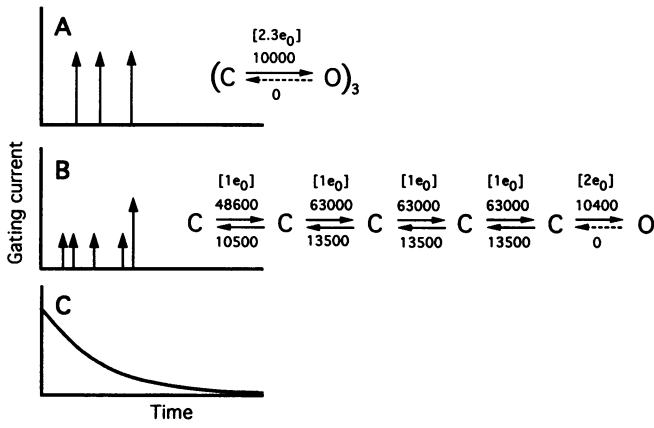


FIGURE 1 Examples of microscopic gating currents. (A) Single-channel gating currents in a Hodgkin-Huxley-like channel having three identical, independent charge movements. (B) A channel having a sequential activation scheme in which four small charge movements are followed by a single large one. (C) Average current from many channels. Rate constants are in units of  $s^{-1}$ ; with the values shown, the two schemes give very similar average time courses. The rate constants shown for the scheme in B are those obtained by Armstrong and Gilly (1979) for the activation pathway of squid  $Na^+$  channels at +10 mV, scaled up by a factor of 4.5. The rate from the open state to the last closed state was set to zero (it would have been  $400 s^{-1}$ ) to match the behavior of the irreversible scheme in A. Although no negative-going current pulses are shown in the illustration in B, they can occur from the four reversible transitions.

We can now write the flux  $\phi_{ij}(t)$ , which is the probability per unit time of a transition from state  $i$  to state  $j$  at time  $t$ , as the product of the probability of being in state  $i$  at time  $t$ , times the transition rate from  $i$  to  $j$ :

$$\phi_{ij}(t) = p_i(t)q_{ij}, \quad (4)$$

for all  $i \neq j$ . Now we assume that transition from  $i$  to  $j$  occurs instantaneously, so that the current due to a transition is an impulse. The time integral of this current is equal to the charge  $\gamma_{ij}$  that is moved in the transition. The mean current due to transitions from  $i$  to  $j$  will then be  $\gamma_{ij}$  times the flux from  $i$  to  $j$ . Summing over all pairs of states we obtain an expression for the total mean gating current from a single channel,

$$\mu(t) = \sum_{i,j} \gamma_{ij} \phi_{ij}(t). \quad (5)$$

## Autocovariance

To derive the autocovariance, let us consider the first term on the right hand side of Eq. 2, the expectation value of the product of  $I$  at two times. There are two cases to consider. First, when  $t_1 = t_2$  we will be considering the correlation of impulses of current with themselves; this results in a term containing a delta function in  $t_2 - t_1$ . Second, there will in general be correlations in the probability of a transition  $i \rightarrow j$  at  $t_1$  with a transition  $k \rightarrow l$  at  $t_2$ . The sum of these two contributions yields

$$\begin{aligned} \langle I(t_1)I(t_2) \rangle = & \sum_{i,j} \phi_{ij}(t_1) \gamma_{ij}^2 \delta(t_2 - t_1) \\ & + \sum_{i,j,k,l} \phi_{ij}(t_1) \gamma_{ij} p'_{jk}(t_2 - t_1) q_{kl} \gamma_{kl}. \end{aligned} \quad (6)$$

The delta-function term is scaled by the rate  $\phi_{ij}$  of transitions and the square of the charge carried in the transitions. The second term is the current due to each possible transition  $i \rightarrow j$  times the current due to transitions  $k \rightarrow l$  conditional on the  $i \rightarrow j$  transition. The current of the  $i \rightarrow j$  transition is simply  $\phi_{ij}(t_1) \gamma_{ij}$  as in Eq. 5. The conditional probability function  $p'_{jk}(t_2 - t_1)$  is the probability of the channel being in state  $k$  at  $t_2$  given that it was in state  $j$  at  $t_1$ . The current from the  $k \rightarrow l$  transitions is then given by the probability for being in  $k$ , times the product of the transition rate and the charge movement  $q_{kl} \gamma_{kl}$ .

To obtain the probability functions, let us consider the general solution to the matrix equation (3). The solution can be written as

$$\mathbf{p}(t) = \mathbf{p}(0)\Omega(t), \quad (7)$$

where  $\Omega(t) = e^{\mathbf{Q}t}$  is the “fundamental matrix” with elements  $\omega_{ij}(t)$ . With this notation the probability of being in a given state is

$$p_i(t) = \sum_j p_j(0) \omega_{ji}(t), \quad (8)$$

and the conditional probability of being in state  $k$  at an interval  $\tau$  after the system is in state  $j$ ,

$$p'_{jk}(\tau) = \omega_{jk}(\tau). \quad (9)$$

Finally, to write an expression for the autocovariance we combine Eqs. 2, 4, 5, and 6 to obtain

$$\begin{aligned} C(t_1, t_2) = & \sum_{i,j} p_i(t_1) q_{ij} \gamma_{ij}^2 \delta(t_2 - t_1) \\ & + \sum_{i,j,k,l} p_i(t_1) q_{ij} \gamma_{ij} q_{kl} \gamma_{kl} [p'_{ik}(t_2 - t_1) - p_k(t_2)]. \end{aligned} \quad (10)$$

Note that this can be written as two terms,

$$C(t_1, t_2) = f(t_1) \delta(t_2 - t_1) + g(t_1, t_2), \quad (11)$$

a delta-function term and a “correlation term”  $g(t_1, t_2)$ . In classical, stationary shot noise arising from a Poisson process of impulses (Schottky, 1918; Rice, 1954) the correlation term is zero. This is because, in a stationary Poisson process, the conditional and unconditional probabilities of events are equal and time-independent. In Eq. 10 this would lead to

$$p'_{ik}(t_2 - t_1) - p_k(t_2) = 0.$$

## Filtering

Since the autocovariance contains a delta function, its form is very sensitive to the kind of filtering that is performed on the measured signal. Let  $h(t)$  be the impulse response of the entire recording system. Then the mea-

sured gating current  $\tilde{I}$  is related to the actual current according to

$$\tilde{I}(t) = \int_{-\infty}^{\infty} I(t - \tau)h(\tau) d\tau, \quad (12)$$

i.e., the convolution of  $I(t)$  with  $h(t)$ . The mean of the filtered current,  $\tilde{\mu}(t)$  is given by a similar convolution. From Eq. 12 it can be shown that the autocovariance of the filtered signal is given by a double convolution (Papoulis, 1965, p. 434),

$$\tilde{C}(t_1, t_2) = \int_{-\infty}^{\infty} \int_{-\infty}^{\infty} C(t_1 - \tau_1, t_2 - \tau_2)h(\tau_1)h(\tau_2) d\tau_1 d\tau_2. \quad (13)$$

In general one must compute the autocovariance in this way. However, assuming that the functions  $f$  and  $g$  of Eq. 11 are slowly varying compared with  $h(t)$  one can make the approximation

$$\tilde{C}(t_1, t_2) \simeq f(t_1) \int_{-\infty}^{\infty} \int_{-\infty}^{\infty} \delta(t_1 - \tau_1 - t_2 + \tau_2) \times h(\tau_1)h(\tau_2) d\tau_1 d\tau_2 + g(t_1, t_2),$$

which, by integrating the delta function, becomes

$$\tilde{C}(t_1, t_2) \simeq f(t_1) \int_{-\infty}^{\infty} h(\tau_1)h(t_2 - t_1 + \tau_1) d\tau_1 + g(t_1, t_2). \quad (14)$$

From this approximation one obtains a useful expression for the variance,

$$\tilde{\sigma}^2(t) = \tilde{C}(t, t) \simeq 2Bf(t) + g(t, t), \quad (15)$$

where  $B$ , which has the dimensions of frequency and is the "effective" filter bandwidth, is given by

$$B = \frac{1}{2} \int_{-\infty}^{\infty} h^2(t) dt \quad (16)$$

## Numerical implementation

### Computation of probability functions

The matrix exponential in Eq. 7 is readily evaluated for an  $n$ -state scheme by first computing the eigenvalues  $\lambda_i$  and the matrix of eigenvectors  $\mathbf{M}$  of  $\mathbf{Q}$ , for example using the QR algorithm (Press et al., 1986). Then one can write

$$\mathbf{Q} = \mathbf{M}\mathbf{\Lambda}\mathbf{M}^{-1},$$

where  $\mathbf{\Lambda}$  is the diagonal matrix with elements  $\Lambda_{ii} = \lambda_i$ , for  $i = 1$  to  $n$ . It then follows, according to Dirac's theorem,

$$\Omega(t) = e^{\mathbf{Q}t} = \mathbf{M}e^{\mathbf{\Lambda}t}\mathbf{M}^{-1},$$

where  $e^{\mathbf{\Lambda}t}$  is the diagonal matrix with diagonal elements  $e^{\lambda_i t}$ , for  $i = 1$  to  $n$ . Consequently, the conditional proba-

bility  $p'_{jk}(\tau)$  (Eq. 9) can be written as a sum of  $n$  exponentials

$$p'_{jk}(\tau) = \sum_{i=1}^n m_{ji}m_{ik}^{-1}e^{\lambda_i\tau} \quad \lambda_i \leq 0, \quad (17)$$

where  $m_{ji}$  and  $m_{ik}^{-1}$  are elements of  $\mathbf{M}$  and its inverse, respectively. Similarly, the probability to be in state  $i$  at time  $t$  (Eq. 8) becomes

$$p_i(t) = \sum_{j=1}^n p_j(0) \sum_{k=1}^n m_{jk}m_{ki}^{-1}e^{\lambda_k t}.$$

For computing the time course of the current and covariance we found it useful to compute and store the  $p_i(t)$  and the matrix  $p'_{jk}(t)$  for each of the 100–400 time points in our calculations. The evaluation of  $C(t_1, t_2)$  then involved looking up the appropriate values and inserting them into Eq. 10.

### Digital filter

For the calculations we used a finite-impulse-response digital filter. Letting  $h$  be the impulse response of the filter and  $f_s$  the sampling frequency, the filtered gating current (Eq. 12) computed at  $t = k/f_s$  becomes

$$\tilde{I}(k) = \sum_{j=-n_c}^{n_c} h(j)I(k-j), \quad (18)$$

where  $n_c$  is the number of filter coefficients used. Similarly, the discrete analogue of Eq. 13, computed at  $t_1 = k_1/f_s$  and  $t_2 = k_2/f_s$ , is

$$\tilde{C}(k_1, k_2) = \sum_{i=-n_c}^{n_c} \sum_{j=-n_c}^{n_c} C(k_1 - i, k_2 - j)h(i)h(j). \quad (19)$$

The filter used in the calculations was a Gaussian filter (Colquhoun and Sigworth, 1983) which provides a good approximation to the high order Bessel analog filter used by Conti and Stühmer. For this filter the impulse response is

$$h(k) = \frac{1}{\sqrt{2\pi}\sigma_f} \exp\left(-\frac{k^2}{2\sigma_f^2}\right),$$

where the width parameter  $\sigma_f$  is related to the  $-3$  db frequency  $f_c$  by

$$\sigma_f = \frac{\sqrt{\ln 2}}{2\pi} \frac{f_s}{f_c},$$

and the number of coefficients was taken to be  $n_c = 4\sigma_f$ . For a Gaussian filter the evaluation of Eq. 16 yields  $B \simeq 1.064 f_c$ .

## Examples

### Irreversible two-state scheme

Suppose a channel makes irreversible transitions from closed state 0 to open state 1 with the rate  $q_{01} = \alpha$  and charge movement  $\gamma_{01} = \gamma$ .

$$C \xrightarrow[\gamma]{\alpha} 0.$$

If the channel is closed at time 0 the probability of the channel being in the closed state at time  $t$  is

$$p_0(t) = e^{-\alpha t},$$

and, since  $q_{10} = 0$ , the mean gating current is

$$\mu(t) = \gamma \alpha e^{-\alpha t}.$$

The autocovariance function is

$$C(t_1, t_2) = \alpha \gamma^2 e^{-\alpha t_1} \delta(t_2 - t_1) - \alpha^2 \gamma^2 e^{-\alpha(t_1+t_2)}. \quad (20)$$

The delta function term decays with the same time course as the mean current. The correlation term is negative and has the property that it depends only on the sum  $t_1 + t_2$ . Fig. 2 shows an example of the filtered covariance. The delta-function term results in a high ridge along the line  $t_1 = t_2$ , while the correlation term produces an exponentially-climbing "floor".

Eq. 15 can be used to approximate the variance, giving

$$\tilde{\sigma}^2(t) \approx 2B\gamma\mu(t) \left[ 1 - \frac{\mu(t)}{2B\gamma} \right].$$

If the gating current arises from the activity of  $N$  independent gates, all translocating the same charge  $\gamma$ , the mean current  $\mu_N$  and autocovariance  $\tilde{C}_N$  are both  $N$  times the one-gate values given above, and the variance versus mean current relation becomes (Conti and Stühmer, 1989)

$$\tilde{\sigma}^2(t) \approx 2B\gamma\mu(t) \left[ 1 - \frac{\mu(t)}{2BN\gamma} \right]. \quad (21)$$

### General two-state scheme

Consider a two-state channel with a nonzero reverse rate  $\beta$ ,

$$C \xrightleftharpoons[\beta]{\alpha} O.$$

Again we take the charge transferred to be  $\gamma$  and assume the channel is in state  $C$  at  $t = 0$ . Then

$$\mu(t) = \gamma \alpha e^{-(\alpha+\beta)t}$$

and

$$C(t_1, t_2) = f(t_1) \delta(t_2 - t_1) + a_1 e^{-(\alpha+\beta)|t_1-t_2|} + a_2 e^{-(\alpha+\beta)(t_1+t_2)}, \quad (22)$$

where

$$f(t_1) = \frac{\gamma^2 \alpha}{\alpha + \beta} [2\beta + (\alpha - \beta) e^{-(\alpha+\beta)t_1}]$$

$$a_1 = -\alpha\beta\gamma^2$$

$$a_2 = -\alpha^2\gamma^2.$$

As in the case of the irreversible two-state scheme, here the correlation term contains a component that decays

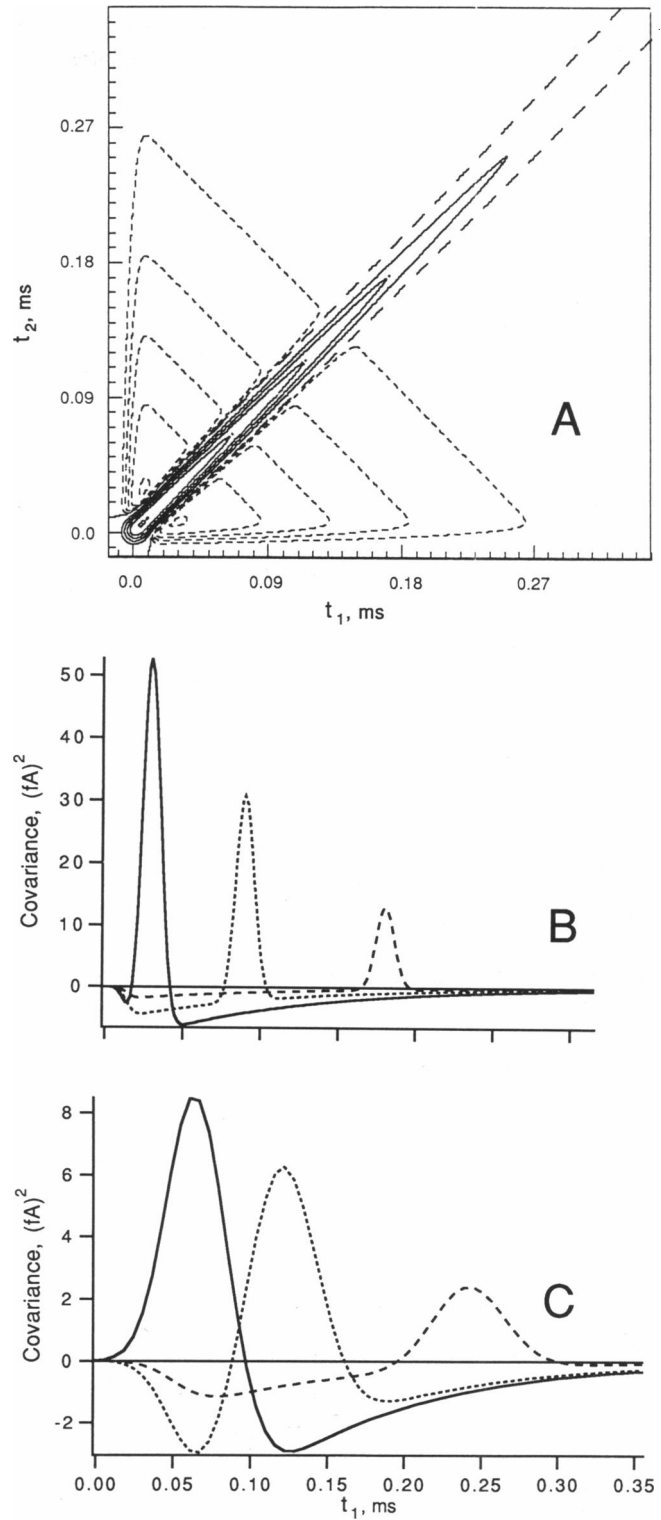


FIGURE 2 Filtered autocovariance from an irreversible two-state scheme. The charge movement  $\gamma = 2e_0$  and decay rate  $\alpha = 10^4 \text{ s}^{-1}$  were assumed. A Gaussian filter having  $f_c = 32 \text{ kHz}$  and a delay of  $15 \mu\text{s}$  was applied. (A) Contour plot of the filtered covariance  $\tilde{C}(t_1, t_2)$ . Positive contours are shown as solid curves, the zero contour as dashed curves, and negative contours are dotted. (B) The filtered covariance plotted as a function of  $t_1$  for  $t_2 = 30 \mu\text{s}$  (solid curve),  $90 \mu\text{s}$  (dotted) and  $180 \mu\text{s}$  (dashed curve). (C) Similar plots of  $\tilde{C}(t_1, t_2)$  but with the filter frequency  $f_c = 8 \text{ kHz}$ , for  $t_2 = 60, 120, \text{ and } 240 \mu\text{s}$ .

exponentially in  $t_1 + t_2$ . However, it also contains a component that decays with the absolute value of the time difference. This component reflects fluctuations that can occur at equilibrium. Defining the time difference  $t = t_2 - t_1$ , we can obtain the stationary autocovariance in the limit of large  $t_1 + t_2$  as

$$C(t) = \frac{\alpha\beta\gamma^2}{\alpha + \beta} [2\delta(t) - (\alpha + \beta)e^{-(\alpha+\beta)|t|}]. \quad (23)$$

The corresponding single-sided power spectrum (Lüger, 1978), obtained as the Fourier transform, is

$$S(f) = 2\gamma^2\alpha\beta\tau \frac{(2\pi f\tau)^2}{1 + (2\pi f\tau)^2},$$

where

$$\tau = \frac{1}{\alpha + \beta}.$$

## RESULTS

### Comparison of variance-mean relationships

We now turn to the question, can measurements of gating current noise discriminate among models of gating in sodium channels? Conti and Stühmer found that the assumption of independent two-state gates (as would for example be found in standard Hodgkin-Huxley kinetics) described their data adequately. On the other hand, there are more complicated schemes that are well supported by experimental data; a well constrained scheme is that of Armstrong and Gilly (1979) which describes the time courses of both ionic current and gating current in the squid axon Na channel. More recently, Vandenberg and Bezanilla (1991) have presented a similar scheme based on single-channel measurements as well. The kinetics of mammalian brain sodium channels are probably quite different from the squid channels (Aldrich and Stevens, 1987); nevertheless, we consider here the Armstrong and Gilly model as an example of an alternative to the two-state model. The two models imply very different physical pictures of the gating process. On the basis of the two-state model, Conti and Stühmer suggest that there are three "gates" each with a valence of 2.3 in the sodium channel. Armstrong and Gilly present a coupled sequence of five transitions; the first four have a valence of 1 and the last step has a valence of 2.

The specific schemes are illustrated in Fig. 1. The rate constants of the six-state scheme are those given by Armstrong and Gilly for the activation steps of their model at a membrane potential of +10 mV, but scaled up by a factor of 4.5. This scaling matches the time course of the mean gating current very well to the 100- $\mu$ s decay observed by Conti and Stühmer at +20 mV. We made the scheme irreversible by setting the rate constant returning from the open state (which would have been 400  $s^{-1}$ ) to

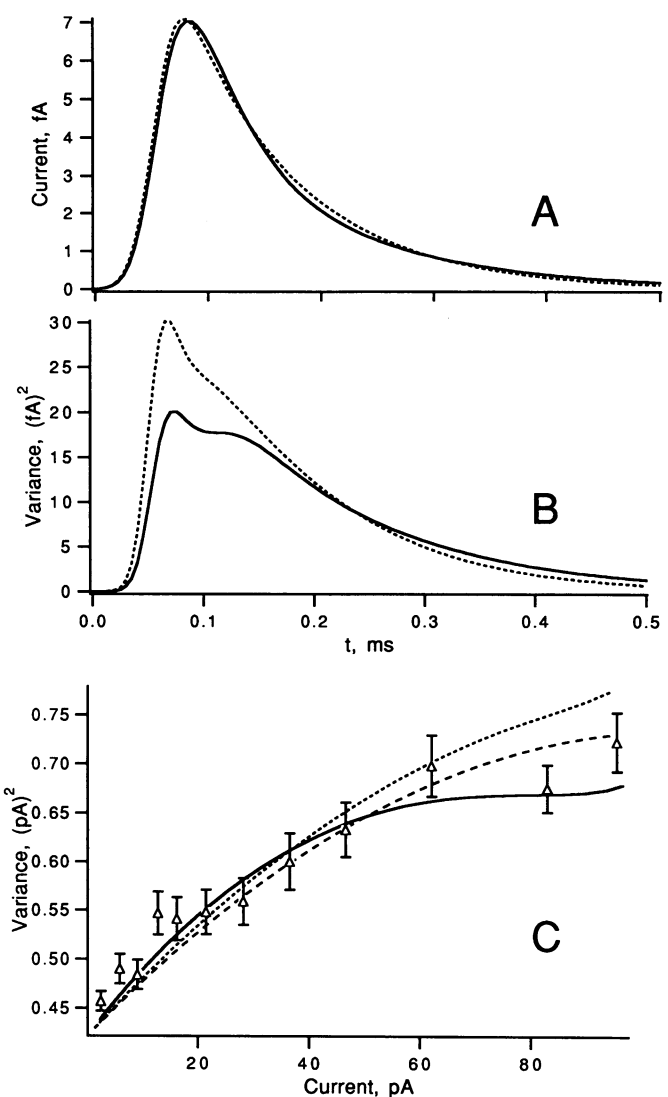


FIGURE 3 Comparison of mean and variance for the two-state and six-state schemes of Fig. 1, *A* and *B*. (*A*) Mean current from the two-state scheme (*dotted curve*) with  $\gamma = 2.3e_0$ , and from the six-state scheme (*solid curve*) with  $\gamma = e_0$  for the first four transitions and  $\gamma = 2e_0$  for the final  $C \rightarrow O$  transition. The current (and variance) from the two-state scheme were scaled up by the factor  $N = 2.61$  to match the total charge movement ( $6e_0$ ) of the six-state scheme. Currents were computed with an 8 kHz Gaussian filter having 60  $\mu$ s delay. (*B*) Corresponding time courses of the variance. (*C*) Variance-mean relationships for the two-state (*dotted curve*) and six-state model (*solid curve*). The relationship is plotted only from the falling phases of the corresponding functions in *A* and *B*. Mean and variance values were scaled by  $N = 3650$  (for the two-state model) or  $N = 1400$  (six-state model) to match the total experimental charge movement of 13.3 fC. Experimental data (*points*) are replotted from Fig. 3 of Conti and Stühmer (1979). The dashed curve is the approximate relationship (Eq. 21) computed with their parameters  $B = 8$  kHz,  $\gamma = 2.3e_0$ , and the total charge movement  $N_\gamma = 13.3$  fC.

zero; this allows a better comparison with the irreversible two-state scheme. With a filter bandwidth of 8 kHz (the same as used in Conti and Stühmer's experiments) the time courses of the mean current (Fig. 3 *A*) predicted by the two models are very similar.

The time courses of the variance (Fig. 3 B) differ substantially, with the six-state model giving lower variance at early times. A difference of this sort is expected if we consider the delta-function term of Eq. 10: it has the same dependence on  $t_1$  as the mean current  $\mu(t)$  except that it is weighted by the square of the valences  $\gamma_{ij}$ , rather than simply the valences themselves. In the two-state model the valence is 2.3, while in the six-state model the transitions that occur at early times all have a valence of unity, resulting in relatively lower variance.

It is interesting to note that, for each model, the variance rises more quickly to a peak than the mean current does, and gives the impression of an overshoot. This effect arises from non-obvious properties of the two-dimensional filtering operation (Eq. 13) which are most apparent at low bandwidths.<sup>1</sup>

Figure 3 C compares the variance-mean relationships of the two models with Conti and Stühmer's data. Also shown in the figure is the approximate variance-mean relationship (Eq. 21) that Conti and Stühmer used for fitting the data. First, let us compare the approximate relationship with our calculation of the mean and variance from the two-state model. The approximation assumes that the correlation term is slowly varying compared with the time resolution set by the filter; its result (the dashed curve in the figure) is seen to differ somewhat from the explicit calculation (*dotted curve*) for the same two-state scheme. This is perhaps to be expected since the filter bandwidth  $B = 8,000$  Hz is not very large compared with the decay rate  $\alpha = 10^4$  s<sup>-1</sup>.

Second, it can be seen from the figure that the variance-mean relationship of the six-state model (*solid curve*) describes the experimental data essentially as well as the two-state model. This is surprising since no parameters were varied to fit the model to the variance-mean relationship itself: the model was adjusted only to match the time course and amplitude of the mean gating current. With adjustment of more parameters, we expect that the six-state model or many other complex gating models could fit the data very well. At this point, how-

<sup>1</sup> The effect can be understood from the nature of the functions  $f(t_1)$  and  $g(t_1, t_2)$  in Eq. 11. For the models considered here these are well approximated by step functions in the neighborhood of  $t_1 = 0$  and  $t_2 = 0$ . Substitution of Eq. 11 into Eq. 13 and integration of the delta function yields the filtered variance

$$\begin{aligned} \tilde{\sigma}^2(t) = & \int_{-\infty}^t f(t-\tau)h(\tau) d\tau \\ & + \int_{-\infty}^t \int_{-\infty}^t g(t-\tau_1, t-\tau_2)h(\tau_1)h(\tau_2) d\tau_1 d\tau_2, \end{aligned}$$

where the upper limits of integration reflect the fact that  $f$  and  $g$  are zero whenever their arguments are negative. The range of integration of the first term increases linearly with  $t$ , while the area of integration in the second increases as  $t^2$ . The result is that, for  $t$  small compared with the width of the filter kernel  $h$ , the first term, which is positive, rises relatively quickly to a peak; the second, negative term rises later and produces the subsequent dip in the time course.

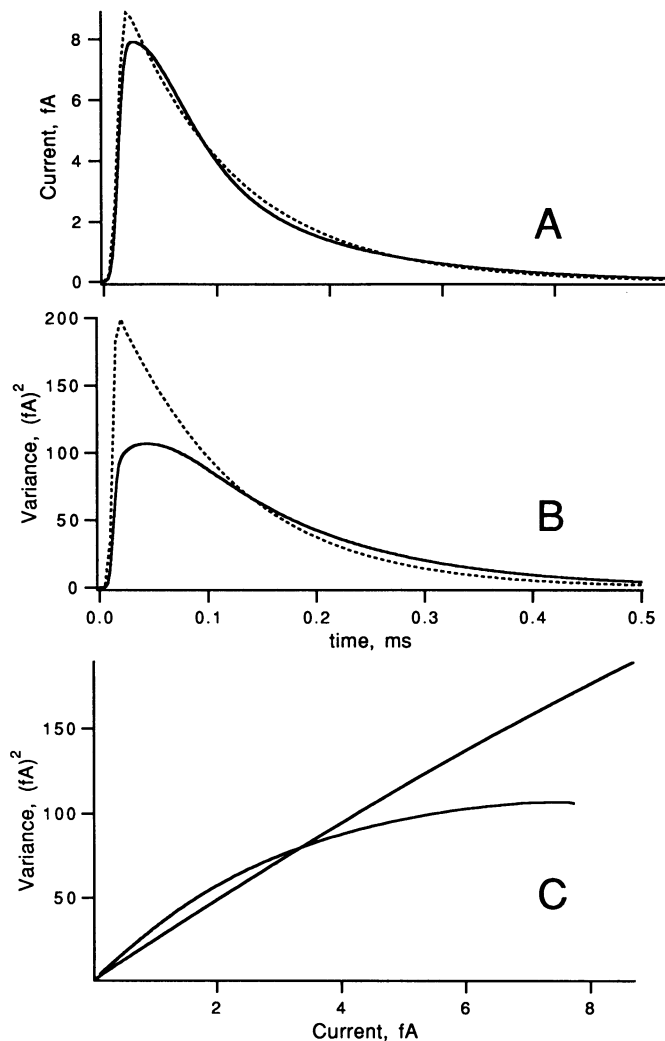


FIGURE 4 Mean and variance for the two-state (*dotted curves*) and six-state schemes, as in Fig. 3, but computed for 32 kHz filter bandwidth. (A) Mean gating current. (B) Corresponding time courses of variance. (C) Variance-mean relationship for the falling phase of the gating current. In each part of the figure the mean and variance for the two-state scheme were scaled up by the factor  $N = 2.61$  to give the same total charge movement of  $6e_0$  as in the six-state scheme.

ever, we conclude only that the data can distinguish only poorly between the two-state and six-state models we used.

### Limit of high bandwidth

The difficulty in distinguishing the two models in this case arises largely from the limited time resolution due to the filtering of the experimental data. When computed for the case of four-fold greater bandwidth (Fig. 4), the variance-mean relationships predicted by the models become more distinct. Variance-mean data obtained at high bandwidth have the additional advantage that their interpretation is also much simpler. From Eq. 15 one observes that with large bandwidth  $B$  the delta-function

term predominates over the correlation term, so that in the limit the variance approaches the simple form

$$\tilde{\sigma}(t) \simeq B \sum_{i,j} \gamma_{ij}^2 p_i(t) q_{ij}, \quad (24)$$

which is very similar to the expression for the mean current, combining Eqs. 4 and 5,

$$\mu(t) = \sum_{i,j} \gamma_{ij} p_i(t) q_{ij}. \quad (25)$$

Here, both the variance and the mean are sums over the fluxes among the states, weighted either by  $\gamma_{ij}^2$ , in the case of the variance, or by  $\gamma_{ij}$  in the case of the mean. Thus, if each of the charge movements  $\gamma_{ij}$  is either equal to the same value  $\gamma$  or else zero, then the variance will be proportional to the mean, with a proportionality factor of  $B\gamma$ . This is obviously the case for the two-state scheme, and at 32 kHz bandwidth (Fig. 4 C) the proportionality holds well.

The six-state scheme has different values for the  $\gamma_{ij}$ : the early steps in the scheme involve smaller charge movements than the later steps. At high bandwidth the variance is therefore seen to be relatively small at early times (*solid curve* in Fig. 4 B). The curvature in the variance-mean relationship (Fig. 4 C) therefore reflects the different-sized charge movements occurring at different times.

### Significance of the autocovariance

The autocovariance function contains much more information than the variance time course alone, and is likely to be useful in discriminating among models for the origin of gating currents. For example, the autocovariance for the six-state model (Fig. 5) shows qualitative differences from that of the two-state model (Fig. 2). The diagonal "ridge" reflects the form of the delta-function term and is best characterized at large bandwidths as discussed above. The "floor" of the autocovariance reflects the correlation term, which is very different in the two models considered here. In the irreversible two-state model the correlation term is negative and arises from the time course of the mean current, depending only on the quantity  $t_1 + t_2$ . In the six-state model the correlation term has additional components due to temporal correlations of successive charge movements in the scheme. These are the terms involving  $p_{ik}$  in Eq. 10, and are mostly positive. For example, the transition from state  $C_0$  to  $C_1$  will be correlated with the transition  $C_1 \rightarrow C_2$ . Since some of the transitions in the scheme are reversible, negative correlations can also occur, e.g., between the transitions  $C_0 \rightarrow C_1$  and  $C_1 \rightarrow C_0$ . The result is a very different form for the "floor" of the autocovariance function.

The effect of heavy filtering on the time course of the variance can be understood from considering the form of the autocovariance function. The variance is given by the points along the diagonal of the autocovariance. Fil-

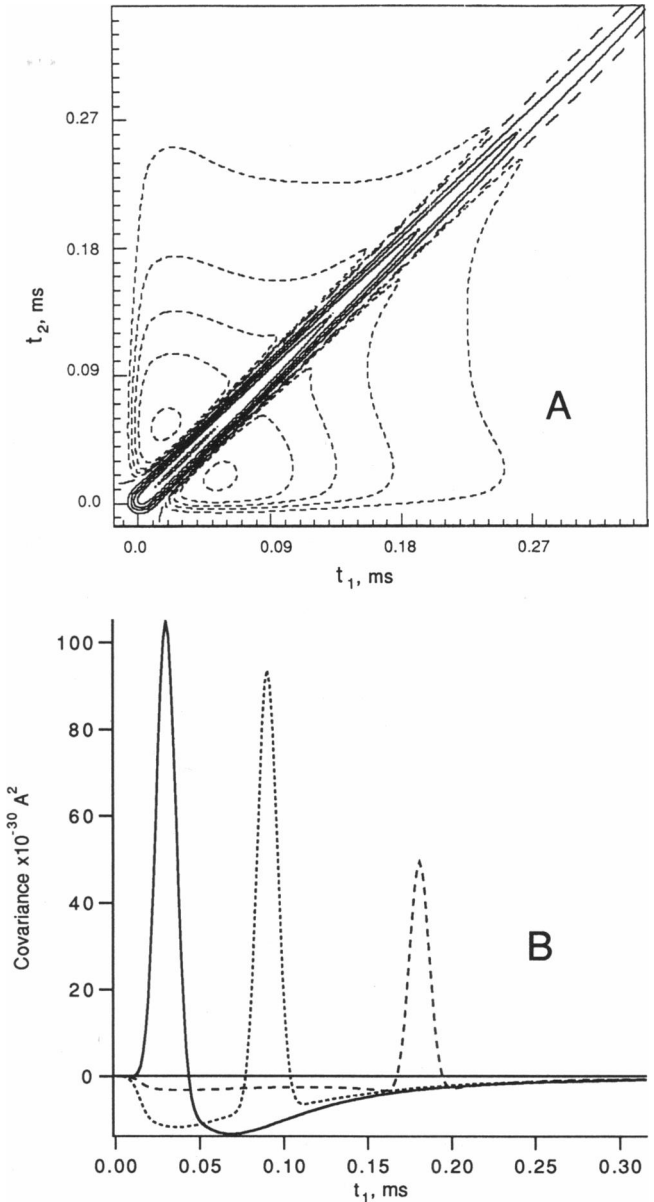


FIGURE 5 Filtered autocovariance from the six-state scheme of Fig. 1 B. A Gaussian filter having  $f_c = 32$  kHz and a delay of  $15 \mu\text{s}$  was applied. (A) Contour plot of the filtered covariance  $\tilde{C}(t_1, t_2)$ . Positive contours are shown as solid curves, the zero contours appear as dashed lines parallel to the diagonal, and negative contours are dotted. (B) Selected sections through the surface shown in A. The autocovariance  $\tilde{C}(t_1, t_2)$  is plotted as a function of  $t_1$  with  $t_2$  fixed at 30, 90, and 180  $\mu\text{s}$  (*solid, dotted, and dashed curves, respectively*).

tering smears out the covariance function in both dimensions (see Eq. 13) having the effect of reducing the contribution of the delta-function peak and thus increasing the relative contribution of the correlation term. Now consider a scheme in which two charge movements of magnitude  $\gamma$  occur in rapid succession. These will give rise to a positive correlation term that will increase the value near the diagonal. At sufficiently low bandwidth, the autocovariance, and also the variance, will be indistinguishable from those of a similar scheme in which

there is a single step carrying a charge movement of  $2\gamma$ . An example of this sort is worked out in the Appendix.

## DISCUSSION

In this paper we have demonstrated the calculation of the variance and autocovariance of nonstationary “shot noise” fluctuations such as those arising in gating currents, and have applied this to experimental data obtained by Conti and Stühmer (1989) from sodium channels expressed in *Xenopus* oocytes. We find that, with the rapid kinetics of the gating current and the time resolution that was available, it is difficult to distinguish between a simple two-state model and a multistate model on the basis of the variance-mean relationship. Better discrimination among models could be made with data obtained with wider bandwidth, and by considering the full autocovariance function.

It should be kept in mind that Conti and Stühmer’s variance measurements at 8 kHz bandwidth represent a remarkable achievement. The main difficulty in acquiring data at wider bandwidths is the magnitude of the background noise. In macro-patch recordings the dominant noise source at high frequencies arises from the series combination of the pipette access resistance  $R_a$  and the patch capacitance  $C_p$ . The background noise spectral density from this source is, for  $R_a C_p f \ll 1$ ,

$$S_b(f) \simeq 4k_B T R_a (2\pi f C_p)^2,$$

where  $k_B$  and  $T$  are Boltzmann’s constant and the absolute temperature, respectively. Typical values are  $C_p = 1$  pF, which corresponds to a patch area of  $\simeq 100$  ( $\mu\text{m}$ )<sup>2</sup>, and  $R_a = 1$  M $\Omega$ . At  $f = 10^4$  Hz, the resulting spectral density  $S_b = 6 \times 10^{-29}$  A<sup>2</sup>/Hz is larger than that expected from either the patch-clamp amplifier or the pipette glass. This spectral density is however roughly equal to that from Poisson shot noise

$$S_I = 2I\gamma,$$

when the mean current  $I = 100$  pA and elementary charge movement  $\gamma = 2e_0$ . Because  $S_b$  increases as  $f^2$ , it will be almost an order of magnitude larger than  $S_I$  at  $f = 30$  kHz. Small changes in the variance  $\sigma_I^2$  due to gating currents of this magnitude can nevertheless be resolved in the presence of a large background variance  $\sigma_b^2$  if a very large number of recordings can be made. To obtain estimates of  $\sigma_I^2$  having the relative standard error  $\epsilon$  one requires an ensemble of

$$N_s \simeq \frac{2}{\epsilon^2} \left[ 1 + \left( \frac{\sigma_b^2}{\sigma_I^2} \right)^2 \right]$$

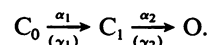
sweeps for the estimation of the variance. Taking  $\epsilon = 0.1$  one obtains  $N_s \simeq 400$  when the gating-current and background variances are equal, but some 24,000 sweeps are required when the background variance is an order of magnitude larger. Other strategies for improving the sig-

nal-to-noise ratio include increasing the density of channels (which would allow the current to increase without increasing  $C_p$  and therefore  $S_b$ ) and using channels having slower kinetics (e.g., K<sup>+</sup> channels) where the recording bandwidth need not be as large.

Conti and Stühmer pointed out that a relatively model-independent measure of the size of elementary charge movements can be made from the variance-mean relationship of gating currents, given the assumption that the filtering of the signal allows sufficient time resolution. However, when the filter bandwidth is limited a rapid succession of small charge movements can become indistinguishable from a single large charge movement. We find that the kinetic scheme of Gilly and Armstrong, which has charge movements of only 1 or  $2e_0$  but has multiple rapid transitions, was able to fit the “on” gating current data shown in Fig. 3 C as well as does the two-state model considered by Conti and Stühmer. It should be noted, however, that Conti and Stühmer were also able to fit the variance-mean relationship of “off” gating current transients with the same model and value for the charge movement. The particular six-state model that we have used here might not be able to reproduce this result for the “off” currents. Nevertheless, we suggest that the figure of  $2.3e_0$  obtained for the two-state model might not reflect the true size of the elementary charge movements, because it could represent the sum of charge movements that occur relatively rapidly in the gating process of the channel.

## APPENDIX

We present here expressions for the mean gating current and the variance for a three-state, irreversible scheme:



Let us assume that the charge moved during the first step  $C_0$  to  $C_1$  is  $\gamma_1$  and the charge moved during the second step  $C_1$  to  $O$  is  $\gamma_2$ . If the channel is in state  $C_0$  at time 0, the probabilities of the channel being in states  $C_0$ ,  $C_1$  and  $O$  at time  $t$  are

$$p_0(t) = e^{-\alpha_1 t}$$

$$p_1(t) = \frac{\alpha_1}{\alpha_2 - \alpha_1} [e^{-\alpha_1 t} - e^{-\alpha_2 t}]$$

$$p_2(t) = 1 + \frac{\alpha_1}{\alpha_2 - \alpha_1} e^{-\alpha_2 t} - \frac{\alpha_2}{\alpha_2 - \alpha_1} e^{-\alpha_1 t}$$

Using Eqs. 4 and 5, we derive the mean current as

$$\mu(t) = \left[ \alpha_1 \gamma_1 + \frac{\alpha_1 \alpha_2}{\alpha_2 - \alpha_1} \gamma_2 \right] e^{-\alpha_1 t} - \frac{\alpha_1 \alpha_2}{\alpha_2 - \alpha_1} \gamma_2 e^{-\alpha_2 t}.$$

The autocovariance function can be explicitly derived from Eq. 11. Its delta-function term is the difference of two exponentials, while the correlation term is a sum of five exponentials of  $t_1$  and  $t_2$ . The approximate filtered variance, assuming that the correlation term is slowly varying (i.e., the limit of large  $B$ ) is obtained from Eq. 15, as

$$\tilde{\sigma}^2(t) \simeq \left[ 2B \left( \alpha_1 \gamma_1^2 + \frac{\alpha_1 \alpha_2}{\alpha_2 - \alpha_1} \gamma_2^2 \right) + \alpha_1 \alpha_2 \gamma_1 \gamma_2 \right] e^{-\alpha_1 t} - 2B \frac{\alpha_1 \alpha_2}{\alpha_2 - \alpha_1} \gamma_2^2 e^{-\alpha_2 t} - [\mu(t)]^2.$$

An interesting special case is when  $\gamma_1 = \gamma_2 = \gamma$ , where

$$\tilde{\sigma}^2(t) \simeq 2B\gamma\mu(t) \left[ 1 - \frac{\mu(t)}{2B\gamma} \right] + \gamma^2 \alpha_1 \alpha_2 e^{-\alpha_1 t}. \quad (26)$$

Notice that the relation between variance and mean current is different from that obtained for the two-state scheme (Eq. 21). The correlation term introduced in the autocovariance leads to a non-parabolic behavior of the variance versus mean current relationship.

Let us consider three special cases for the behavior of this scheme. First, if  $\alpha_1 \gg B \gg \alpha_2$ , then the first transition is so rapid that it is not resolved. The resolvable behavior is essentially that due to the second step, so that after the initial impulse of current the system behaves essentially like the irreversible two-state scheme with rate  $\alpha_2$ . A second case is when  $\alpha_1 = 2\alpha_2$  and  $\gamma_1 = \gamma_2$ . With these parameters the three-state scheme is strictly equivalent to two independent two-state schemes with parameters  $\alpha_2$  and  $\gamma_2$ .

Finally, it is instructive to consider the situation  $\alpha_1 \ll \alpha_2$ . In this case the second transition proceeds rapidly after the first transition occurs. The first step is rate-limiting, so that

$$\mu(t) \simeq \alpha_1 [\gamma_1 + \gamma_2] e^{-\alpha_1 t},$$

and the effective valence approaches the sum ( $\gamma_1 + \gamma_2$ ). For  $B \gg \alpha_1$  the variance is

$$\tilde{\sigma}^2(t) \simeq \frac{2B(\gamma_1^2 + \gamma_2^2) + \alpha_2 \gamma_1 \gamma_2}{\gamma_1 + \gamma_2} \mu(t) - [\mu(t)]^2,$$

which can be rewritten as

$$\tilde{\sigma}^2(t) \simeq 2B\gamma\mu(t) \left[ 1 - \frac{\mu(t)}{2B\gamma} \right]$$

with

$$\gamma = \frac{\gamma_1^2 + \gamma_2^2 + \alpha_2 \gamma_1 \gamma_2 / 2B}{\gamma_1 + \gamma_2}.$$

We thank Drs. F. Conti and W. Stühmer for helpful comments on early versions of the manuscript.

This work was supported by National Institutes of Health grant NS-21501.

Received for publication 7 April 1992 and in final form 6 October 1992.

## REFERENCES

1. Aldrich, R. W., and C. F. Stevens. 1987. Voltage-dependent gating of single sodium channels from mammalian neuroblastoma cells. *J. Neurosci.* 7:418-431.
2. Armstrong, C. M., and W. F. Gilly. 1979. Fast and slow steps in the activation of sodium channels. *J. Gen. Physiol.* 74:691-711.
3. Colquhoun, D., and A. G. Hawkes. 1977. Relaxation and fluctuations of membrane currents that flow through drug-operated ion channels. *Proc. R. Soc. Lond. B* 199:231-262.
4. Colquhoun, D., and F. J. Sigworth. 1983. Fitting and statistical analysis of single-channel records. In *Single Channel Recording*. B. Sakmann and E. Neher, editors. Plenum Press, New York. 191-263.
5. Conti, F., and W. Stühmer. 1989. Quantal charge redistributions accompanying the structural transitions of sodium channels. *Eur. Biophys. J.* 17:53-59.
6. Frehland, E. 1978. Current noise around steady states in discrete transport systems. *Biophys. Chem.* 8:255-265.
7. Frehland, E. 1982. Stochastic Transport Processes in Discrete Biological Systems. Lecture Notes in Biomathematics, Vol. 47. Springer-Verlag, Berlin. 169 pp.
8. Läuger, P. 1978. Transport noise in membranes. Current and voltage fluctuations at equilibrium. *Biochim. Biophys. Acta.* 507:337-349.
9. Heinemann, S. H., and F. J. Sigworth. 1990. Open channel noise V. Fluctuating barriers to ion entry in gramicidin A channels. *Biophys. J.* 57:499-514.
10. Papoulis, A. 1965. Probability, Random Variables, and Stochastic Processes. McGraw-Hill, New York. 538 pp.
11. Press, W. H., B. P. Flannery, S. A. Teukolsky, and W. T. Vetterling. 1986. Numerical Recipes. The Art of Scientific Computing. Cambridge University Press, Cambridge. 818 pp.
12. Rice, S. O. 1954. Mathematical analysis of random noise. In *Selected Papers on Noise and Stochastic Processes*. N. Wax, editor. Dover Publications Inc., New York. 133-183.
13. Schottky, W. 1918. Über spontane Stromschwankungen in verschiedenen Elektrizitätsleitern. *Ann. Phys. (Leipzig).* 57:541-567.
14. Vandenberg, C. A., and F. Bezanilla. 1991. A sodium channel gating model based on single channel, macroscopic ionic, and gating currents in the squid giant axon. *Biophys. J.* 60:1511-1533.